

A Determination of the Corrosion and Microstructure Properties of AlSi10Mg Material Produced by Different Direct Metal Laser Sintering (DMLS) Process Parameters

Mustafa Safa YILMAZ^{1*}

¹Fatih Sultan Mehmet Vakıf University, ALUTEAM
(ORCID: [0000-0003-2614-9121](https://orcid.org/0000-0003-2614-9121))



Keywords: Additive Manufacturing, Direct Metal Laser Sintering (DMLS), Parameter optimization, Corrosion, AlSi10Mg.

Abstract

Additive Manufacturing (AM) has been developing with increasing interest recently. The development of this technology will accelerate with the increase in material, process, and product quality. It is therefore essential to investigate these shortcomings of additive manufacturing products. In this study, the microstructure and corrosion properties of the material (AlSi10Mg) were investigated by changing the production parameters in the Direct Metal Laser Sintering (DMLS) process. Energy density was considered in parameter selection. Depending on the process parameters, the corrosion, topography, and mechanical properties of the DMLS-AlSi10Mg material were investigated in detail. It has been determined that the corrosion resistance and hardness of the material are directly related to porosity.

1. Introduction

The advantages of Additive Manufacturing (AM) are that it can construct complex-shaped parts without the need for other processes [1][2][3][4]. Powder bed fusion (PBF) technologies are the most popular processes for metal AM technologies that are called selective laser melting (SLM), direct metal laser sintering (DMLS), and electron beam melting (EBM) [5][6][7]. DMLS uses the layer-by-layer production of metallic parts and semifinished products directly from the metal powders [8] [9] [10]. The DMLS system has many advantages: the production of complex parts (according to casting or rolling), no need for expensive tools required in production, a low amount of sawdust and waste, a cost advantage in low-numbered production, and accessibility to the final product within hours [11] [12]. AlSi10Mg alloy is generally used in pressure casting. Since this alloy has a ratio close to its eutectic composition, it has high fluidity and low shrinkage [13]. Due to these advantages, the most widely used alloy in Additive Manufacturing is AlSi10Mg alloy. AlSi10Mg alloy

produced with AM is widely used in automotive, marine, medical, and aerospace [14] [15] [16].

Many parameters must be controlled in additive manufacturing technologies. The slightest change in parameters can cause severe deterioration or improvement in the material. As a result of the parametric changes, changes in the energy values are loaded into the DMLS system. This energy value creates significant differences in the materials, and many studies are ongoing on this subject [5] [17] [18] [19].

As a result of production parameters, kinetic effects such as segregations, dislocations, and residual stresses in the material cause changes in the material's mechanical and corrosion properties. In addition, if the production parameters are not well optimized, more serious defects such as porosity and cracks may occur in the material. This study examines the difference in the power and scan speed values (effect the energy density) used by the system and the change in the microstructure, surface properties, and corrosion properties.

*Corresponding Author: m.safayilmaz@gmail.com

Received: 13.04.2022, Accepted: 25.09.2022

2. Material and Method

The productions were made with AlSi10Mg alloy powders, and its chemical analysis (Table 1) and SEM picture (Figure 1) were given.

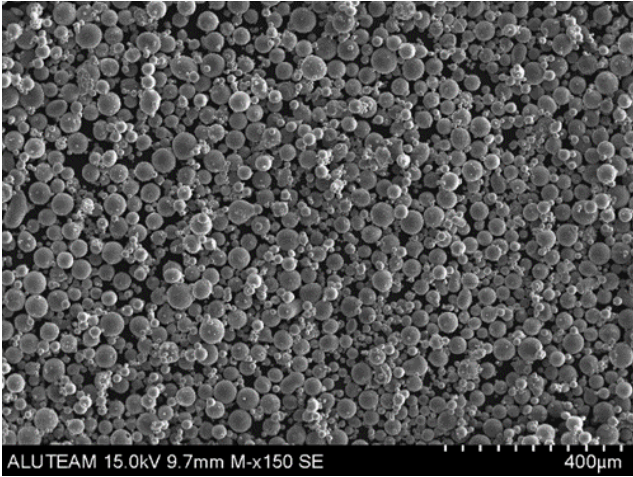


Figure 1. AlSi10Mg metal powder SEM image.

Table 1. AlSi10Mg powder’s chemical analysis (wt.%), d50 = 35±5 µm

Si	Fe	Mn	Cu	Ni	Zn	Mg	Sn	Al
9-11	≤0.55	≤0.45	≤0.05	≤0.05	≤0.10	0.2-0.45	≤0.05	Other

Table 2. AlSi10Mg powder’s chemical analysis (wt.%), d50 = 35±5 µm

Sample	Laser power (P, Watt)	Scan Speed (v, mm/s)	Energy input (E*, joule)
E1	150	1000	26.31
E2	370	1600	40.57
E3	250	1000	43.85
E4	370	1000	64.91
E5	370	600	108.18
E6**	370	1300	49.93

**DMLS AlSi10Mg manufacturing standard parameters.

$$E=P/(v.h.t)$$

The specimens were manufactured with 40x15x5 mm (x-y-z) size via the EOS M290 DMLS machine. X-ray diffraction (XRD)-(Bruker D8), Scanning electron microscopy (SEM) - (Hitachi SU3500), optical microscopy (OM), Hardness test (Shimadzu Vickers hardness device (HV 0.05)), corrosion analysis (IVIUM/Vertex-CompactStat), surface roughness measurement (Mitutoyo SJ210) and porosity measurement methods (ImageJ) were used for characterization analysis.

Before corrosion investigation, specimens were physically polished with SiC pare and diamond suspension (1 micron), washed with acetone and dried. Potentiodynamic polarization experiments were applied at 0.5 mV/s and 25 °C in an aerated 3.5

The details of parameter design, which is the focus of the study, are given in Table 2 and show the changes in energy density with different laser power and speed. Increasing the scanning speed and scanning distance increases the production speed, while low values of these two parameters cause an increase in energy density. In this study, the effect of scanning speed was investigated by keeping the scanning distance constant. In addition, different values of laser power were tried to change the energy density. While manufacturing, some parameters were kept constant (0.19 mm hatch distance (h), 30 µm Layer thickness (t)), and the scan lines of every layer within the core region were rotated by 67° concerning the previous layer’s scan lines. In addition, the formula used to calculate the energy density is given in Table 2. How different parameters affect the energy can be seen here.

wt% NaCl solution. The surface area was 1 cm², and open-circuit potential (OCP) was stabilized for 1800 s before potentiodynamic tests.

3. Results and Discussion

The phases of the produced samples were examined (Figure 2). As can be seen from the spectral results, no elements other than aluminium and silicon were detected in the internal structure, and an amorphous phase was not formed.

The relation between the energy input level and the roughness is given in Figure 3. Surface roughness measurements (10 measurements were

made) were made from the laser trace surfaces of each sample. It is seen that the surface roughness values are directly influenced by the energy input [5] [20] [21] [22] [23]. Surface roughness is also high with a high energy input parameter (E5). With the same scanning speed but increasing in laser power experiments (the increase in laser power increases the energy), the roughness value increased (E1, E3, E4).

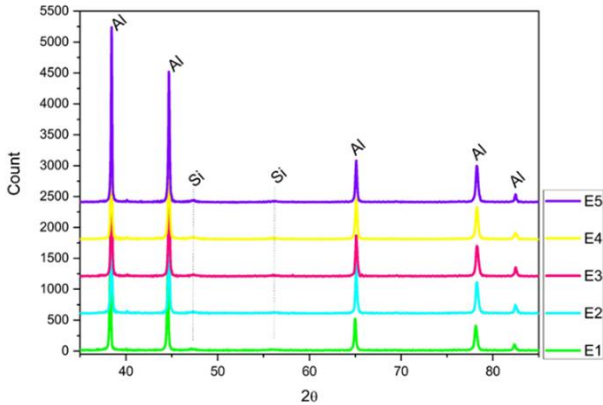


Figure 2. XRD results of additively manufactured samples.

The results of the inner porosity (15 measurements were made from the optical images with the ImageJ software program) are given in Figure 4. Many parameters in additive manufacturing systems affect the amount of porosity in the material's internal structure [23]. This study investigated the effect of the change in the amount of energy. Pore formation in additive manufacturing changes with many parameters. Although the energy levels are close (E2, E3, E6), there are differences in the amount of porosity in different parameters from the standard parameter (E6). This situation shows the importance of optimum power and laser speed in production. When the total energy amount is low (E1), the powder material does not melt and remains a void in the structure. In cases where energy is high (E5), gas gaps are trapped in the melt pool due to the evaporation effect [17][21][24][25].

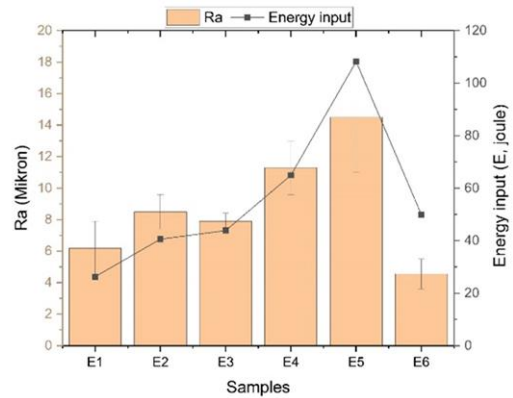


Figure 3. Energy input and surface roughness results of samples

Although they have different laser power and scanning speeds, minimum porosity levels were obtained in samples with values close to optimum energy levels (E3 and E2).

The hardness values of the samples produced with different parameters and without any heat treatment are shared in Figure 4. The mechanical properties of the material are directly related to the porosity in the structure [14] [21] [26]. It is seen that the hardness values are proportional to the internal porosity ratio of the samples.

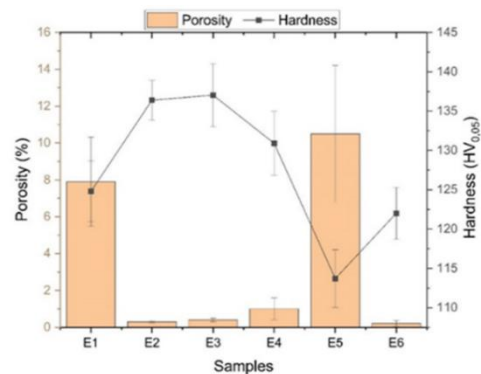


Figure 4. Hardness and porosity results of samples

It is known that there are microstructure changes in additive manufacturing products with changing process parameters [27] [28] [29]. As shown in Figure 5, an optical microscope study was carried out, and gas evaporation and lack of fusion errors are visible. Gas evaporation formation (E5) occurs due to the high energy input. On the other hand, a lack of fusion errors occurs due to insufficient energy (E1) or slow scanning speeds [27] [28] [30].

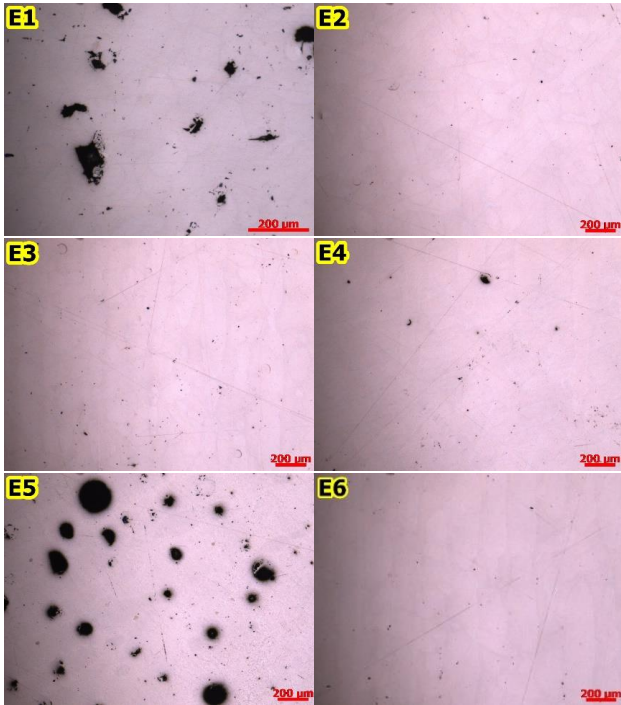


Figure 5. Optical images of samples

Table.3 and Figure 6 were given to examine the corrosion properties of the material. It is E_{cor}

Table 3. Corrosion results of samples

Sample	E_{cor} (V)	I_{cor} ($\mu A/cm^2$)	Corrosion rate (mm/year)	Polarization resistance (k Ω)
E1	-0.6936	1.84	0.0006035	1.31
E2	-0.6925	0.40	0.0003696	8.23
E3	-0.7535	1.12	0.0003664	4.24
E4	-0.7053	1.21	0.0003984	4.94
E5	-0.7457	2.82	0.0009231	2.76
E6	-0.7213	0.47	0.0005389	9.98

Surface SEM images share corrosion formation details (Figure 7). The corrosion rate was higher in the samples with a high porosity value, which is expected. It contains the electrochemical solution of the cavities in the material and creates regional differences in concentration and pH [33]. As a result of this difference, the material erosion is higher than the surfaces without porosity [34]. The surface SEM images show that corrosion is more active around the voids in the material.

Further corrosion of E1, E4 and E5 samples is explained in this way. It is expected that less corrosion is observed in the E6 sample (the standard production parameter for the DMLS system), and the E2 and E3 parameters showed similar corrosion properties. The corrosion intensity on the surfaces of E1, E4 and E5 samples, which contain more porosity, is visible.

(corrosion potential), which shows the thermodynamic resistance of the material against oxidation [31] [32]. A high E_{cor} value indicates that the material starts to corrode later. The I_{cor} value represents the progression rate of corrosion. The relationship was determined between the porosity values of the material and the corrosion resistance (Table.3 and Figure 6).

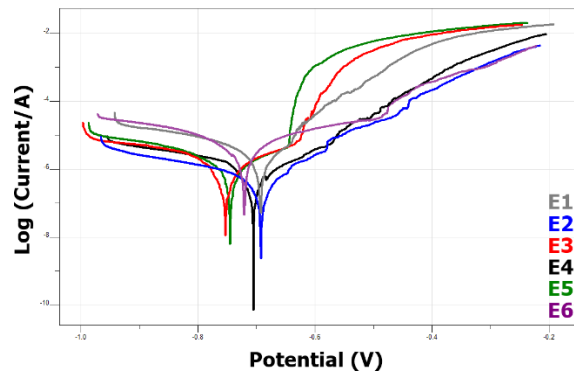
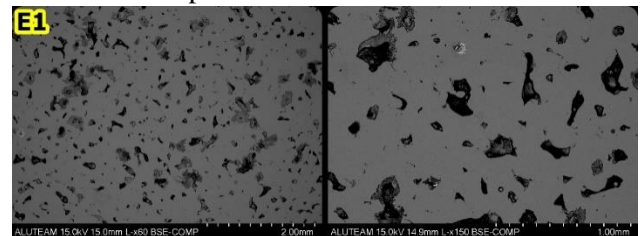
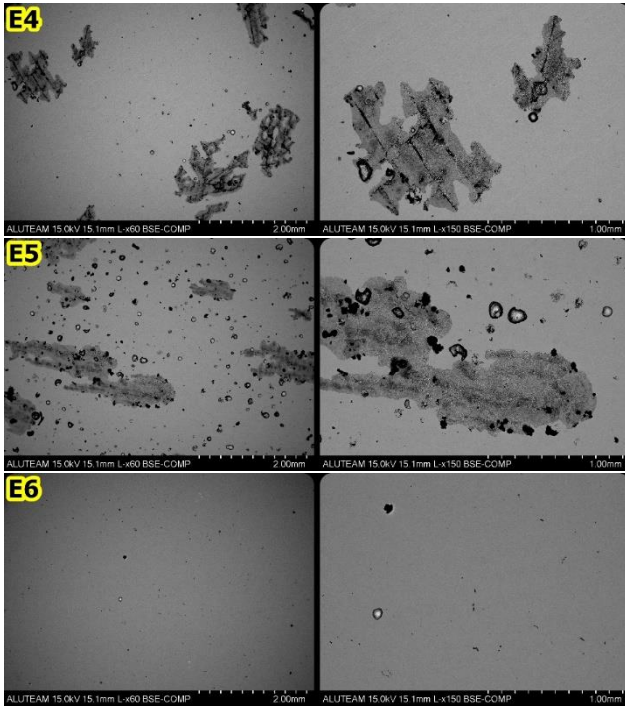


Figure 6. Corrosion (Tafel polarization) graphs of the samples

Corrosion properties can vary according to the material's internal structure features. One of these properties is the amount of internal stress. It is known that the corrosion rate increases as the internal stress in the material increases. It is thought that the high amount of energy in production and the high internal stress are also effective in accelerating corrosion in E5 and E4 samples.





Fatih Sultan Mehmet Vakif University Aluminum Test Training and Research Center is supported by Istanbul Development Agency (ISTKA) and T.R. Ministry of Development.

Figure 7. Corrosion (Tafel polarization) surfaces SEM images of the samples

I_{cor} values of the materials were determined by calculating from the graphics in Figure.6. A low I_{cor} value indicates that the material is more resistant to corrosion. It is seen that the surface corrosion images in Figure.7 and I_{cor} values support each other.

4. Conclusion and Suggestions

The results obtained from the investigation can be listed as follows;

- With the process parameter change, different phases did not occur in the material, and even peak shift and expansion behaviours were not observed in the results.
- A direct relationship was determined between the energy used in the system and the surface roughness.
- The porosity values in the material increased with the energy density being too high or too low. It has been determined that different kinetics occur in these changes.
- Although there is no direct effect of the process parameter on the hardness values, it has been observed that it is seriously related due to the porosity in the structure.
- It has been determined that the material's corrosion resistance is directly related to the porosity level in the structure.

Acknowledgement

References

- [1] Maamoun, A.H., Elbestawi, M., Dosbaeva, G.K., Veldhuis, S.C., “Thermal post-processing of AlSi10Mg parts produced by Selective Laser Melting using recycled powder”. *Addit. Manuf.* 21, 234–247 (2018). <https://doi.org/10.1016/j.addma.2018.03.014>
- [2] Domröse, R., Grünberger, T., “Identification of process phenomena in DMLS by optical in-process monitoring”. (2015)
- [3] Pantělejev, L., Štěpánek, R., Koutný, D., Paloušek, D., “Mechanical properties of AlSi10Mg alloy processed by SLM”. *Mater. Eng. - Mater. inžinierstvo.* 24, 108–114 (2018)
- [4] Yusuf, S.M., Gao, N., “Influence of energy density on metallurgy and properties in metal additive manufacturing”. *Mater. Sci. Technol.* (United Kingdom). 33, 1269–1289 (2017). <https://doi.org/10.1080/02670836.2017.1289444>
- [5] Thijs, L., Montero Sistiaga, M.L., Wauthle, R., Xie, Q., Kruth, J.P., Van Humbeeck, J., “Strong morphological and crystallographic texture and resulting yield strength anisotropy in selective laser melted tantalum”. *Acta Mater.* (2013). <https://doi.org/10.1016/j.actamat.2013.04.036>
- [6] Buchbinder, D., Meiners, W., Wissenbach, K., Poprawe, R., “Selective laser melting of aluminum die-cast alloy—Correlations between process parameters, solidification conditions, and resulting mechanical properties”. *J. Laser Appl.* 27, S29205 (2015). <https://doi.org/10.2351/1.4906389>
- [7] Zakay, A., Aghion, E., “Effect of Post-heat Treatment on the Corrosion Behavior of AlSi10Mg Alloy Produced by Additive Manufacturing”. *Jom.* 71, 1150–1157 (2019). <https://doi.org/10.1007/s11837-018-3298-x>
- [8] Palumbo, B., Del Re, F., Martorelli, M., Lanzotti, A., Corrado, P., “Tensile properties characterization of AlSi10Mg parts produced by direct metal laser sintering via nested effects modeling”. *Materials* (Basel). 10, (2017). <https://doi.org/10.3390/ma10020144>
- [9] Krishnan, M., Atzeni, E., Canali, R., Calignano, F., Manfredi, D., Ambrosio, E.P., Iuliano, L., “On the effect of process parameters on properties of AlSi10Mg parts produced by DMLS”. *Rapid Prototyp. J.* 20, 449–458 (2014). <https://doi.org/10.1108/RPJ-03-2013-0028>
- [10] Trevisan, F., Calignano, F., Lorusso, M., Pakkanen, J., Aversa, A., Ambrosio, E.P., Lombardi, M., Fino, P., Manfredi, D., “On the selective laser melting (SLM) of the AlSi10Mg alloy: Process, microstructure, and mechanical properties”. *Materials* (Basel). 10, (2017). <https://doi.org/10.3390/ma10010076>
- [11] Oter, Z.C., Coskun, M., Akca, Y., Surmen, O., Yılmaz, M.S., Ozer, G., Tarakci, G., Khan, H.M., Koc, E., “Support optimization for overhanging parts in direct metal laser sintering”. *Optik* (Stuttg). 181, 575–581 (2019). <https://doi.org/10.1016/j.ijleo.2018.12.072>
- [12] Herzog, D., Seyda, V., Wycisk, E., Emmelmann, C., “Additive manufacturing of metals”. *Acta Mater.* 117, 371–392 (2016). <https://doi.org/10.1016/j.actamat.2016.07.019>
- [13] Girelli, L., Tocci, M., Gelfi, M., Pola, A., “Study of heat treatment parameters for additively manufactured AlSi10Mg in comparison with corresponding cast alloy”. *Mater. Sci. Eng. A.* 739, 317–328 (2019). <https://doi.org/10.1016/j.msea.2018.10.026>
- [14] Brandl, E., Heckenberger, U., Holzinger, V., Buchbinder, D., “Additive manufactured AlSi10Mg samples using Selective Laser Melting (SLM): Microstructure, high cycle fatigue, and fracture behavior”. *Mater. Des.* (2012). <https://doi.org/10.1016/j.matdes.2011.07.067>
- [15] Ghasri-Khouzani, M., Peng, H., Attardo, R., Ostiguy, P., Neidig, J., Billo, R., Hoelzle, D., Shankar, M.R., “Comparing microstructure and hardness of direct metal laser sintered AlSi10Mg alloy between different planes”. *J. Manuf. Process.* 37, 274–280 (2019). <https://doi.org/10.1016/j.jmapro.2018.12.005>
- [16] Girelli, L., Tocci, M., Montesano, L., Gelfi, M., Pola, A., “Optimization of heat treatment parameters for additive manufacturing and gravity casting AlSi10Mg alloy”. *IOP Conf. Ser. Mater. Sci. Eng.* 264, 0–8 (2017). <https://doi.org/10.1088/1757-899X/264/1/012016>
- [17] Manfredi, D., Calignano, F., Krishnan, M., Canali, R., Ambrosio, E.P., Atzeni, E., “From powders to dense metal parts: Characterization of a commercial alsimg alloy processed through direct metal laser sintering”. *Materials* (Basel). (2013). <https://doi.org/10.3390/ma6030856>
- [18] Kruth, J.P., Mercelis, P., Van Vaerenbergh, J., Froyen, L., Rombouts, M., “Binding mechanisms in selective laser sintering and selective laser melting”. *Rapid Prototyp. J.* 11, 26–36 (2005). <https://doi.org/10.1108/13552540510573365>

- [19] Simchi, A., Direct laser sintering of metal powders: “Mechanism, kinetics and microstructural features”. *Mater. Sci. Eng. A.* (2006). <https://doi.org/10.1016/j.msea.2006.04.117>
- [20] Fox, J.C., Moylan, S.P., Lane, B.M., “Effect of Process Parameters on the Surface Roughness of Overhanging Structures in Laser Powder Bed Fusion Additive Manufacturing”. In: *Procedia CIRP* (2016)
- [21] Greco, S., Gutzeit, K., Hotz, H., Kirsch, B., Aurich, J.C., “Selective laser melting (SLM) of AISI 316L—impact of laser power, layer thickness, and hatch spacing on roughness, density, and microhardness at constant input energy density”. *Int. J. Adv. Manuf. Technol.* (2020). <https://doi.org/10.1007/s00170-020-05510-8>
- [22] Girelli, L., Giovagnoli, M., Tocci, M., Pola, A., Fortini, A., Merlin, M., La Vecchia, G.M., “Evaluation of the impact behaviour of AlSi10Mg alloy produced using laser additive manufacturing”. *Mater. Sci. Eng. A.* 748, 38–51 (2019). <https://doi.org/10.1016/j.msea.2019.01.078>
- [23] Rashid, R., Masood, S.H., Ruan, D., Palanisamy, S., Rahman Rashid, R.A., Elambasseril, J., Brandt, M., “Effect of energy per layer on the anisotropy of selective laser melted AlSi12 aluminium alloy”. *Addit. Manuf.* 22, 426–439 (2018). <https://doi.org/10.1016/j.addma.2018.05.040>
- [24] Wang, D., Yang, Y., Su, X., Chen, Y., “Study on energy input and its influences on single-track, multi-track, and multi-layer in SLM”. *Int. J. Adv. Manuf. Technol.* 58, 1189–1199 (2012). <https://doi.org/10.1007/s00170-011-3443-y>
- [25] Karimi, P., Sadeghi, E., Ålgårdh, J., Andersson, J., “EBM-manufactured single tracks of Alloy 718: Influence of energy input and focus offset on geometrical and microstructural characteristics”. *Mater. Charact.* 148, 88–99 (2019). <https://doi.org/10.1016/j.matchar.2018.11.033>
- [26] Hrabe, N., Quinn, T., “Effects of processing on microstructure and mechanical properties of a titanium alloy (Ti-6Al-4V) fabricated using electron beam melting (EBM), Part 2: Energy input, orientation, and location”. *Mater. Sci. Eng. A.* (2013). <https://doi.org/10.1016/j.msea.2013.02.065>
- [27] Shamsaei, N., Yadollahi, A., Bian, L., Thompson, S.M., “An overview of Direct Laser Deposition for additive manufacturing; Part II: Mechanical behavior, process parameter optimization and control”. *Addit. Manuf.* 8, 12–35 (2015). <https://doi.org/10.1016/j.addma.2015.07.002>
- [28] Aboulkhair, N.T., Everitt, N.M., Ashcroft, I., Tuck, C., “Reducing porosity in AlSi10Mg parts processed by selective laser melting”. *Addit. Manuf.* 1, 77–86 (2014). <https://doi.org/10.1016/j.addma.2014.08.001>
- [29] Kempen, K., Thijs, L., Yasa, E., Badrossamay, M., Verheecke, W., Kruth, J.P., “Process optimization and microstructural analysis for selective laser melting of AlSi10Mg”. *22nd Annu. Int. Solid Free. Fabr. Symp. - An Addit. Manuf. Conf. SFF 2011.* 484–495 (2011)
- [30] Mukherjee, T., Wei, H.L., De, A., DebRoy, T., “Heat and fluid flow in additive manufacturing – Part II: Powder bed fusion of stainless steel, and titanium, nickel and aluminum base alloys”. *Comput. Mater. Sci.* 150, 369–380 (2018). <https://doi.org/10.1016/j.commatsci.2018.04.027>
- [31] Prashanth, K.G., Debalina, B., Wang, Z., Gostin, P.F., Gebert, A., Calin, M., Kühn, U., Kamaraj, M., Scudino, S., Eckert, J., “Tribological and corrosion properties of Al-12Si produced by selective laser melting”. *J. Mater. Res.* (2014). <https://doi.org/10.1557/jmr.2014.133>
- [32] Shahriari, A., Khaksar, L., Nasiri, A., Hadadzadeh, A., Amirkhiz, B.S., Mohammadi, M., “Microstructure and corrosion behavior of a novel additively manufactured maraging stainless steel”. *Electrochim. Acta.* 339, 135925 (2020). <https://doi.org/10.1016/j.electacta.2020.135925>
- [33] Özer, G., Tarakçi, G., Yılmaz, M.S., Öter, Z.Ç., Sürmen, Ö., Akça, Y., Coşkun, M., Koç, E., “Investigation of the effects of different heat treatment parameters on the corrosion and mechanical properties of the AlSi10Mg alloy produced with direct metal laser sintering”. *Mater. Corros.* (2019). <https://doi.org/10.1002/maco.201911171>
- [34] Yılmaz, M.S., Özer, G., Öter, Z.Ç., Ertuğrul, O., “Effects of hot isostatic pressing and heat treatments on structural and corrosion properties of direct metal laser sintered parts”. *Rapid Prototyp. J.* 27, 1059–1067 (2021). <https://doi.org/10.1108/RPJ-10-2020-0245>